Electronic Structures of ANb$_2$PS$_{10}$ (A=Ag, Na) and AuNb$_4$P$_2$S$_{20}$

Bull. Korean Chem. Soc. **2003**, Vol. 24, No. 6   739

Electronic Structures of ANb$_4$PS$_{10}$ (A=Ag, Na) and AuNb$_4$P$_2$S$_{20}$

Dongwoon Jung[*] **and Sung-Jin Kim**[†,*]

Institute of Natural Science and Department of Chemistry, Wonkwang University, Iksan, Jeonbuk 570-749, Korea
[†]Department of Chemistry, Ewha Womans University, Seoul 120-750, Korea

New quaternary compounds ANb$_2$PS$_{10}$ (A = Na, Ag) and AuNb$_4$P$_2$S$_{20}$ were synthesized and characterized. The structures of three compounds consist of one-dimensional infinite chains built by [Nb$_2$S$_{12}$] and [PS$_4$] units. Cation atoms are occupied within the van der Waals gap of sulfur atoms between infinite chains to make $-$S$\cdots$M$^+\cdots$S$-$ contacts. There is only one Au atom site and so crystallographically a unit cell contains four equivalent Au atoms in AuNb$_4$P$_2$S$_{20}$. This is only the half of the numbers of Na or Ag atoms in NaNb$_2$PS$_{10}$ or AgNb$_2$PS$_{10}$. The ratio between Nb$_2$PS$_{10}$ matrix *vs* the cation is, therefore, 1 : 1 for Ag and Na, but it is 2 : 1 for Au. Mixed valency in Au or Nb was expected to balance the charge in the latter compound. The electronic structures calculated based on the extended Huckel tight-binding method show that ANb$_2$PS$_{10}$ (A = Ag, Na) are semiconducting, while AuNb$_4$P$_2$S$_{20}$ is metallic, which is not consistent with the experimental results of these three compounds that all exhibit semiconducting property. The result of calculation suggests that AuNb$_4$P$_2$S$_{20}$ might be a magnetic insulator. Magnetic measurement experiment exactly proved that the compound is a Slater antiferromagnetic material with the Neels' temperature of 45 K. It is recognized, therefore, that electronic structure analysis is very useful to understand the properties of compounds.

Key Words : Mixed valency, Electronic structure, Magnetic insulator

Introduction

Transition metal thiophosphates have been actively investigated due to their structural low-dimensionality and importance as oxidizing host materials for secondary lithium batteries.[1] Early transition metal thiophosphates with various phosphorus-sulfur polyanions [P$_n$Q$_m$]$^{x-}$ and low-dimensional structures have been reported. For example, V$_2$PS$_{10}$ is one-dimensional,[2] VP$_{0.2}$S$_2$, VP$_{0.17}$S$_2$, V$_2$P$_4$S$_{13}$, V$_{0.78}$PS$_3$, V$_2$P$_4$S$_{13}$, AVP$_2$S$_7$, Nb$_2$PS$_{10}$, Nb$_4$P$_2$S$_{21}$ and NbP$_2$S$_8$, are two-dimensional compounds.[3-9] Since the first alkali metal contained compound with [P$_n$Q$_m$]$^{x-}$ units, KNb$_2$PS$_{10}$,[10] is known, recently, we synthesized more family members of one-dimensional quaternary thiophosphates, ANb$_2$PS$_{10}$ (A = Na, Ag)[11] and AuNb$_4$P$_2$S$_{20}$. The structures of ANb$_2$PS$_{10}$ are closely related to that of 2D-Nb$_4$P$_2$S$_{21}$. As already known, Nb$_4$P$_2$S$_{21}$ is two-dimensional compound where $-$S-S-S$-$ bridges connect neighboring one-dimensional chains. However, in ANb$_2$PS$_{10}$ (A = Na, Ag, Au), the $-$S-S-S$-$ bridges are broken and reduced to $-$S-S$-$, and also instead of bridges between chains through $-$S-S$-$, A$^+$ caions are inserted between the chains, thereby forming $-$S$\cdots$M$^+\cdots$S$-$ contacts.

A mixed valence compound contains an element that exhibits two distinctive oxidation states. Crystallographically, the ions having different oxidation states result in two different structures around each of them. A linear AuX$_2$ and a square planar AuX$_4$ (X = Se) for Au$^+$ and Au^{3+}, respec-

tively, are found in Wells' caesium salts.[12-15] In most cases, such a mixed valency occurs in the compound containing transition metals. Whether the mixed valency occurs in AuNb$_4$P$_2$S$_{20}$ which contain two transition metals or not will be interesting to investigate. Herein, the differences in the crystal structures, mixed oxidation states, and electronic structures between in ANb$_2$PS$_{10}$ (A = Na, Ag) and AuNb$_4$P$_2$S$_{20}$ are discussed.

Experimental Section

Synthesis. NaNb$_2$PS$_{10}$ was prepared from the mixture of Na$_2$S (Dukan), Nb powder (Kojundo 99.9%), P$_2$S$_5$ (Fluka >98%) and S powder (Aldrich 99.999%) in a molar ratio of 0.93 : 1 : 3 : 4. AgNb$_2$PS$_{10}$ was prepared from the stoichiometric quantities of Ag powder (Kojima 99.99%), Nb powder, P powder (Aldrich 99.99%) and S powder in a molar ratio of 1 : 2 : 1 : 10. The reacting mixture with total mass of ~1 g was double-sealed in an evacuated quartz tube and heated at 750 °C for 6 days for NaNb$_2$PS$_{10}$ and 900 °C for 2 weeks for AgNb$_2$PS$_{10}$. Then, to obtain single crystals with a suitable size for structure determination, the heated products were slowly cooled to room temperature (2 °C/h). The crystals of AuNb$_4$P$_2$S$_{20}$ were prepared from a mixture of Au powder (Kojima 99.99%), Nb powder (Kojundo 99.9%), P powder (Aldrich 99.99%) and S powder (Aldrich 99.999 %) in a molar ratio of 1 : 2 : 1.1 : 10.3. The reacting mixture was double-sealed in an evacuated quartz tube and heated at 900 °C for 2 weeks. Then, to obtain single crystal with suitable size for structure determination, the heated product was slowly cooled to room temperature (2 °C/h).

Electronic Structure Calculation. Electronic structure

---

[*]Authors to whom correspondence should be addressed. Dong-woon Jung (Tel: +82-63-850-6207; Fax: +82-63-841-4893; E-mail: djung@wonkwang.ac.kr); Sung-Jin Kim (E-mail: sjkim@mm.ewha.ac.kr)

740   *Bull. Korean Chem. Soc.* **2003**, Vol. 24, No. 6

Dongwoon Jung and Sung-Jin Kim

Table 1. Atomic Orbital Parameters Used in Extended Hückel Calculations

Atom	Orbital	H_{ii} (eV)[a]	ζ_1	C_1	ζ_2	C_2
S	3s	-20.0	2.122	1.0		
	3p	-13.3	1.827	1.0		
P	3s	-18.6	1.75	1.0		
	3p	-14.0	1.30	1.0		
Nb	5s	-10.1	1.89	1.0		
	5p	-6.86	1.85	1.0		
	4d	-12.1	4.08	0.6401	1.64	0.5516
Au	6s	-10.92	2.602	1.0		
	6p	-5.55	2.584	1.0		
	5d	-15.076	6.163	0.64418	2.791	0.53558

[a]$H_{ii} = <\chi_i | H^{eff} | \chi_i>$, $i = 1, 2, 3, \ldots$. The value approximated by valence-state ionization potential.

calculations for $AuNb_4P_2S_{20}$ and ANb_2PS_{10} (A = Na, Ag) were performed by the extended Hückel method within the framework of tight-binding approximation.[16] Density of states (DOS) were calculated based on the given crystal structure for 396 k-points. The atomic orbital parameters employed in the calculation were the default values in the CAESAR program,[17] which are listed in Table 1.

X-Ray Photoelectron Spectroscopy. XPS spectra for $AuNb_4P_2S_{20}$ and $AgNb_2PS_{10}$ had been measured with ESCA 2000 electron spectrometer (VG microtech). Pelletized samples were mounted on a aluminium plate. Nonmonochromatic Al $K\alpha$ radiation was used as an excitation source (hν = 1486.6 eV). During the measurement, the spectrometer was pumped to a residual pressure of ~10^{-9} Torr. The data were taken from fresh samples and also after Ar bombardment on surface of palletized samples. The binding energies of gold and niobium in $AuNb_4P_2S_{20}$ and $AgNb_2PS_{10}$ were measured. The 1s binding energy of carbon, 284.6 eV was used as an internal standard.

Electron Transport Measurements. The electrical resistance of a single-crystalline $AuNb_4P_2S_{20}$ was measured using the four-probe method over the temperature 80-300 K.

Magnetic Susceptibility Measurements. Magnetic susceptibility data were recorded on a MPMS5 magnetometer (Quantum Design Inc.). The calibration was made at 298 K using a palladium reference sample furnished by Quantum Design Inc. The data were collected over a temperature range of 15-300 K at a magnetic field of 5000 G and were corrected for diamagnetism.

Results and Discussion

Crystal Structure. The structure of a quaternary thiophosphate $AuNb_4P_2S_{20}$ is similar to those of ANb_2PS_{10} (A = Na, Ag) family except cation position within a one-dimensional chain framework. Figure 1(a) and 1(b) show the crystal structures of $NaNb_2PS_{10}$ and $AuNb_4P_2S_{20}$, which are projected on the ac-plane. The building blocks of the chains are constructed with $[Nb_2S_{12}]$ and $[PS_4]$ units. In $[Nb_2S_{12}]$, each Nb atom is centered in a distorted bicapped trigonal
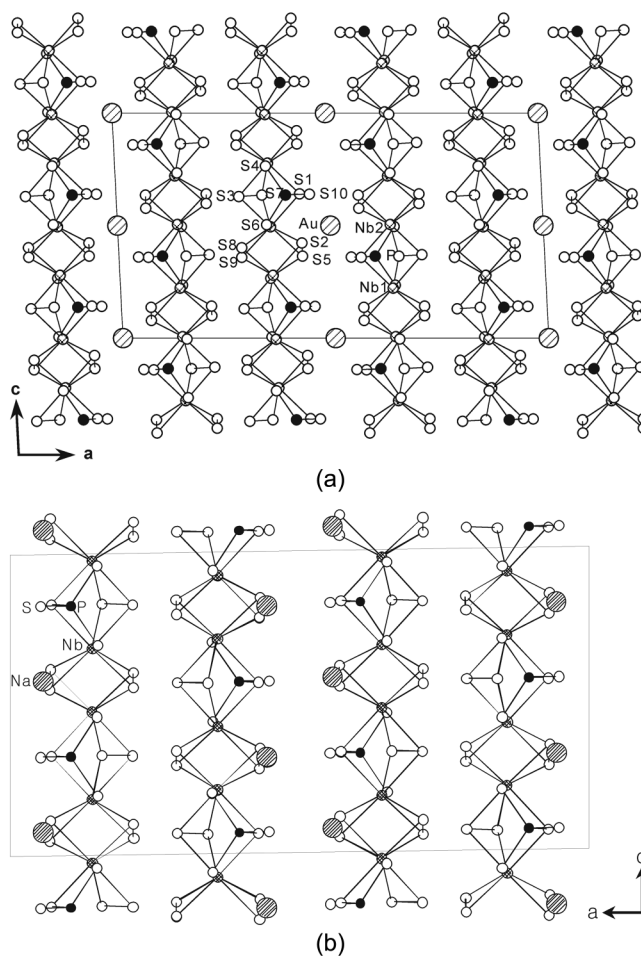

Figure 1. (a) Crystal structure of $AuNb_4P_2S_{20}$ projected along the b-axis, where $^1_\infty[$ $[Nb_2PS_{10}^-]$ chains and a unit cell are shown. (b) Crystal structure of $NaNb_4PS_{10}$ projected along the b-axis.

prism composed of three S_2^{2-} anions. The $[PS_4]$ units are attached to make bridges between two $[Nb_2S_{12}]$ units to make the long Nb-Nb pair. (The short Nb-Nb interactions are found in the $[Nb_2S_{12}]$ unit itself). Accordingly, the short and long Nb-Nb interactions depend on whether there is a $[PS_4]$ unit between the metals or not.

Au atoms are occupied on a special position in $AuNb_4P_2S_{20}$ crystal with inversion symmetry, which is different from in $NaNb_2PS_{10}$ and $AgNb_2PS_{10}$ because Na^+ and Ag^+ cations occupied in the general positions. Au atoms in $AuNb_4P_2S_{20}$ are in close contact with S atoms in the range of 2.305(2)-3.774(2) Å. The results of the A-S (A=Na, Ag, Au) bond distances are exactly inverse of the cation sizes; 116 pm, 129 pm, and 151 pm for Na^+, Ag^+ and Au^+, respectively, when the coordination number is six. Au atom can make a strong
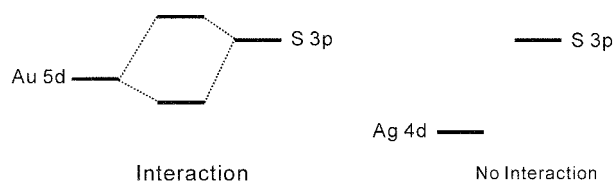
Scheme 1

covalent interaction with S atoms since the energy level of its d-orbital lies close to that of S p-orbital, while the interaction should be weak for Ag atom because of the large energy difference, as briefly shown in Scheme 1. The shortest Au-S(10) contacts at 2.305(2) Å is very close to the linear Au-S contacts found in KAuS, KAuS$_5$ and Na$_3$AuS$_2$.[18-20]

The short and long Nb-Nb interactions are found in ANb$_2$PS$_{10}$ and AuNb$_4$P$_2$S$_{20}$ and the bond lengths are similar to those found in other ternary compounds Nb$_2$PS$_{10}$ and Nb$_4$P$_2$S$_{21}$. The eight Nb-S distances are in the range of 2.466(2) Å-2.624(2) Å with the average bond length of 2.538(2) Å in AuNb$_4$P$_2$S$_{20}$. The average distance of P-S bonds is 2.040(3) Å, which is similar to that of AgNb$_2$PS$_{10}$. There is no notable feature in the Nb-S bond lengths; within error range Nb-S bond lengths are almost the same. In the long run, the different aspects between AuNb$_4$P$_2$S$_{20}$ and ANb$_2$PS$_{10}$ (A=Na, Ag) are the cation-sulfur distance and the number of cations.

The stoichiometry of AuNb$_4$P$_2$S$_{20}$ instead of AuNb$_2$PS$_{10}$ suggests that there might be some higher oxidation states on Au atom or other elements such as Nb atoms. Several Au compounds have been known to show mixed valence states Au^{3+}(d^8) and Au$^+$(d^{10}). The geometry for Au^{3+} is square planar, while that for Au$^+$ is linear. Since there is only one crystallographical position on Au with linear S-Au-S structure in AuNb$_4$P$_2$S$_{20}$, the possibility of mixed valence states on Au is excluded. Instead, there might be some mixed valence states on Nb atoms to compensate for the positive charge in the compound. Consequently, (Au^{1+})[(Nb$_2$S$_6$)$_2$]$^{5+}$ (PS$_4$$^{3-}$)$_2$ scheme seems to be a reasonable suggestion to satisfy the charge neutrality.

XPS Spectra. XPS experiments were carried out to examine the oxidation state of Au and Nb in AuNb$_4$P$_2$S$_{20}$ and the results are listed in Table 2, 3 and 4. The binding energies at 84.4 eV and 88.0 eV are typical indications for Au 4f$_{7/2}$ and 4f$_{5/2}$, respectively, when the Au is mono-

Table 2. Results of Curve Fit to Au 4d Spectrum of AuNb$_4$P$_2$S$_{20}$

Binding energy (eV)	FWHM (eV)	Area (%)	State
84.4	1.20	57.0	4f$_{7/2}$ (Au$^+$)
88.0	1.20	43.0	4f$_{5/2}$ (Au$^+$)

Table 3. Results of Curve Fit to Nb 3d Spectrum of AgNb$_2$PS$_{10}$

Binding energy (eV)	FWHM (eV)	Area (%)	State
203.4	1.17	59.9	3d$_{5/2}$ (Nb^{4+})
206.2	1.17	40.1	3d$_{3/2}$ (Nb^{4+})

Table 4. Results of Curve Fit to Nb 3d Spectrum of AuNb$_4$P$_2$S$_{20}$

Binding energy (eV)	FWHM (eV)	Area (%)	State
203.5	1.14	41.1	3d$_{5/2}$ (Nb^{4+})
206.2	1.14	29.1	3d$_{3/2}$ (Nb^{4+})
207.6	1.15	18.5	3d$_{5/2}$ (Nb^{5+})
210.3	1.15	11.2	3d$_{3/2}$ (Nb^{5+})

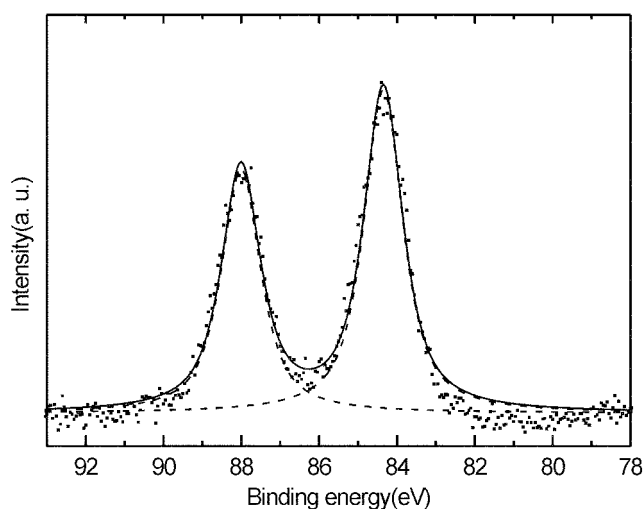**Figure 2**. Au 4f X-ray photoelectron spectrum for AuNb$_4$P$_2$S$_{20}$. The dashed lines are the fitted 4f$_{5/2}$ and 4f$_{7/2}$ curves of Au$^+$, and the solid line is the amount of fitted curves.
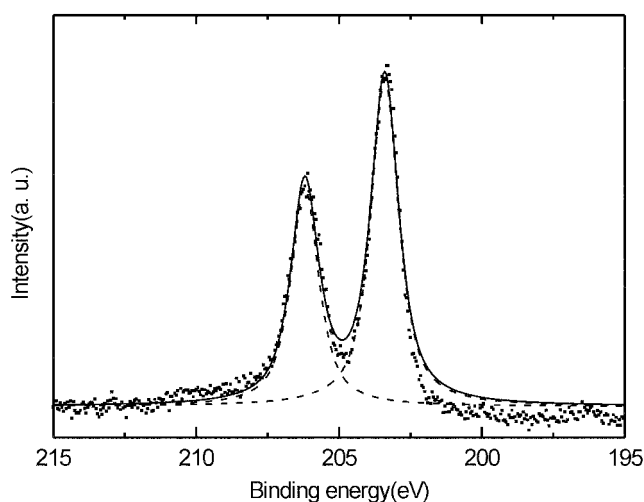

Figure 3. Nb 3d X-ray photoelectron spectrum for AuNb$_4$P$_2$S$_{20}$. The dashed lines are the fitted 3d$_{3/2}$ and 3d$_{5/2}$ curves of Nb^{4+}, and the solid line is the amount of fitted curves.

positive.[21] (see Fig. 2). Any indication of Au^{3+}, whose peak is typically shown at >90 eV is not found. In the long run all Au in AuNb$_4$P$_2$S$_{20}$ can be assigned to be Au$^+$. Figure 3 and 4 show Nb 3d level XPS spectrum of AgNb$_2$PS$_{10}$ and AuNb$_4$P$_2$S$_{20}$, respectively. The Nb 3d level XPS spectrum of AgNb$_2$PS$_{10}$ show doublet at 203.4 eV and 206.2 eV indicating Nb^{4+}.[22] However, the XPS of AuNb$_4$P$_2$S$_{20}$ shows three peaks indicating more than one Nb oxidation state. Since there are two crystallographically different Nb atoms, the oxidation states of the two Nb atoms can be different. The three peaks could be resolved into two pair of Nb 3d$_{3/2}$ and 3d$_{5/2}$. The first doublet at 207.6 eV and 210.3 eV which is left-shifted is assigned to Nb^{5+} and the second doublet appears at the similar binding energy of AgNb$_2$PS$_{10}$ at 203.5 eV and 206.2 eV, therefore, it is assigned to Nb^{4+}.

Electronic Structure. Projected density of states (PDOS) calculated for AgNb$_2$PS$_{10}$ and AuNb$_4$P$_2$S$_{20}$ are shown in

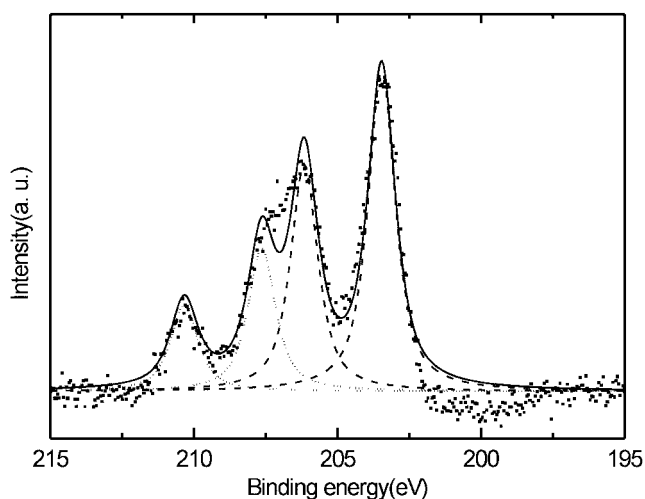**Figure 4**. Nb 3d X-ray photoelectron spectrum for $AuNb_4P_2S_{20}$. The dashed lines are the fitted $3d_{3/2}$ and $3d_{5/2}$ curves of Nb^{4+}, the dotted lines are those of Nb^{5+}, and the solid line is the amount of fitted curves.
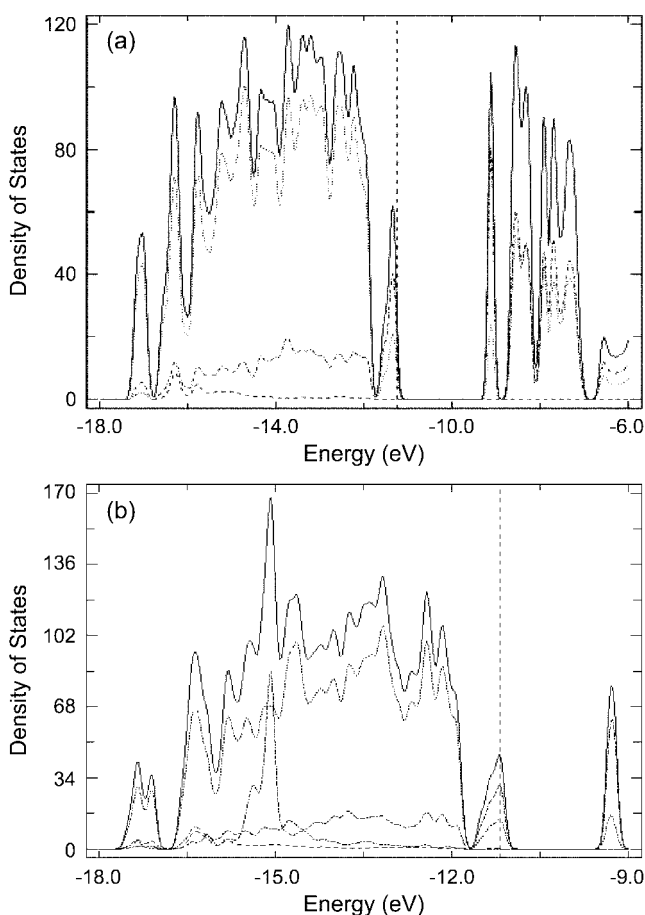

Figure 5. (a) Projected density of states (PDOS) curves calculated for $AuNb_4P_2S_{20}$. The solid line, the dotted line, the dash-dotted line, and the dashed line represent the total DOS, the PDOS of the S 3p, the PDOS of the Nb 4d, and the PDOS of the Au 5d orbitals, respectively. (b) Projected density of states (PDOS) curves calculated for $AgNb_2PS_{10}$. The solid line, the dotted line, the dash-dotted line, and the dashed line represent the total DOS, the PDOS of the S 3p, the PDOS of the Nb 4d, and the PDOS of the Au 5d orbitals, respectively.
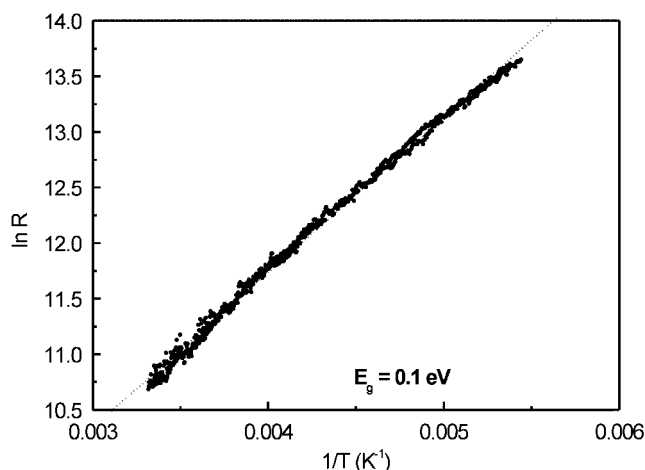

Figure 6. (a) Electrical resistivity data of $AuNb_4P_2S_{20}$ as a function of temperature and (b) that for $AgNb_2PS_{10}$.

Figure 5(a) and 5(b), respectively. $AgNb_2PS_{10}$ and $AuNb_4P_2S_{20}$ are semiconducting and metallic, respectively. PDOS data supports the existence of mixed valence not in Au but in Nb. All Au 5d-orbital lies well below the Fermi level, but Nb 4d-orbital lies below and above the Fermi level, which means that the oxidation states of Au and Nb are +1, and +5, respectively. Rather strong interaction of Au-S is supposed to be the reason why the charge transfer occurs from Nb to Au through the Nb-S-Au contact. Electrons move from Nb 4d to Au 5d since the energy level of Nb 4d is higher than that of Au 5d. Consequently, the mixed valency occurs on Nb (*i.e.*, Nb^{4+} and Nb^{5+}) but not on Au (*i.e.*, Au^+) in $AuNb_4P_2S_{20}$. This result is consistent with the XPS and crystallographical data.

Electron Transport and Magnetic Properties. The temperature dependency of the electrical resistivity for $AuNb_4P_2S_{20}$ is shown in Figure 6. The temperature dependency of the electrical resistivity for $AgNb_2PS_{10}$ and $NaNb_2PS_{10}$ show similar pattern so those are not shown. All showed semiconducting behavior which is not consistent with the result of DOS calculated for $AuNb_4P_2S_{20}$. The metallic property from the DOS in $AuNb_4P_2S_{20}$ might be due to the shortage of electrons donated by the cation (*i.e.*, see the stoichiometries of $AuNb_4P_2S_{20}$ and $AgNb_2PS_{10}$). In the metallic figure, the valence band of $AuNb_4P_2S_{20}$ consists of mainly Nb d-orbital with the d^1 or d^0 electronic configuration according to the mixed valency on Nb. It is well established that the electronic state of a crystalline solid with a partially filled band may not become metallic but insulating so as to minimize electron-electron repulsion (see Scheme 2). Such an insulating state can be magnetic or nonmagnetic depending upon how electron-electron repulsion is minimized. For
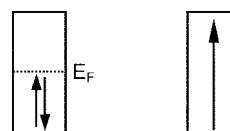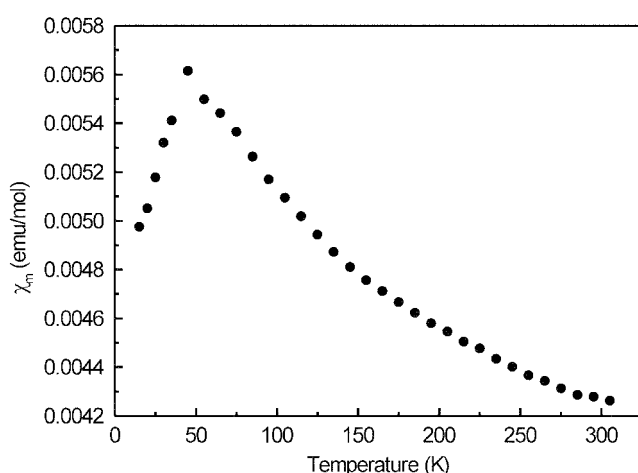

Scheme 2

Figure 7. Plots of molar magnetic susceptibility (χ_m, emu/mol) *vs* temperature (K) for AuNb₄P₂S₂₀.

instance, a magnetic insulating state of the Slater antiferromagnetism introduces spin density alternation at neighboring sites, thus decreasing the on-site electron-electron repulsion. To understand the difference the results of between electronic structure calculation and electron transport measurement, magnetic measurements was performed. The discrepancy between the calculated and experimental results suggests that the compound might be a magnetic insulator. The magnetic susceptibility data in Figure 7 clearly show that AuNb₄P₂S₂₀ illustrates ferromagnetic and antiferromagnetic properties with the Neels temperature (T_N) of 45 K.

Conclusions

The new quaternary compound AuNb₄P₂S₂₀ was prepared and characterized. Since the compound contains fewer cations in a unit cell the role of Nb in AuNb₄P₂S₂₀ is quite different from that of the already known compounds ANb₂PS₁₀ (A=Na, Ag). The oxidation states of Au and Nb in ANb₂PS₁₀ (A=Na, Ag) are +1 and +4, respectively. However, partial amount of Au or Nb should have higher oxidation states to balance the charge in AuNb₄P₂S₂₀. The mixed valency such as Au^{+1} and Au^{+3}, or Nb^{+4} and Nb^{+5}, are, therefore, expected. The XPS data tell us that the mixed valence state arises on Nb atoms not on Au atoms only in AuNb₄P₂S₂₀, which is not found in ANb₂PS₁₀ (A=Na, Ag). This conclusion is consistent with the results of the crystal structure of Au environment and projected density of states (PDOS) data. The discrepancy between the calculated and

experimental results suggests that the compound might be a magnetic insulator. The magnetic susceptibility data clearly show that AuNb₄P₂S₂₀ illustrates ferromagnetic and antiferromagnetic properties with the Neels' temperature (T_N) of 45 K. It is recognized, therefore, that electronic structure analysis is very useful to understand the properties of compounds.

References

1. (a) Thompson, A. H.; Whittingham, M. S. *U. S. Patent 4,049,870*, 1977. (b) Brec, R.; Lemehaute, A. *Fr Patenta 7,704,518 and 4,049,879*, 1977. (c) Nishi, Y. *Electrochemistry* **2000**, *68*, 1008.
2. Brec, R.; Ouvrard, G.; Evain, M.; Grenouilleau, P.; Rouxel, J. *J. Solid State Chem.* **1983**, *47*, 174.
3. Brec, R.; Ouvrard, G.; Freour, R.; Rouxel, J.; Soubeyroux, J. L. *Mater. Res. Bull.* **1983**, *18*, 689.
4. Evain, M.; Brec, R.; Ouvrard, G.; Rouxel, J. *J. Solid State Chem.* **1985**, *56*, 12.
5. Brec, R.; Grenouilleau, P.; Evain, M.; Rouxel, J. *Rev. Chim. Miner.* **1983**, *20*, 295.
6. Brec, R.; Evain, M.; Grenouilleau, P.; Rouxel, J. *Rev. Chim. Miner.* **1983**, *20*, 283.
7. Grenouilleau, P.; Brec, R.; Evain, M.; Rouxel, J. *Rev. Chim. Miner.* **1983**, *20*, 628.
8. Ouvrard, G.; Freour, R.; Brec, R.; Rouxel, J. *Mater. Res. Bull.* **1985**, *20*, 1053.
9. (a) Kopnin, E.; Coste, S.; Jobic, S.; Evain, M.; Brec, R. *Mater. Res. Bull.* **2000**, *35*, 1401. (b) Durand, E.; Evain, M.; Brec, R. *J. Solid State Chem.* **1983**, *102*, 146.
10. Do, J.; Yun, H. *Inorg. Chem.* **1996**, *35*, 3729.
11. Goh, E.-Y.; Kim, S.-J.; Jung, D. *J. Solid State Chem.* **2002**, *168*, 119.
12. Kitagawa, H.; Kojima, N.; Matsushita, N.; Ban, T.; Tsujikawa, I. *J. Chem. Soc., Dalton Trans.* **1991**, 3115.
13. Elliott, N.; Pauling, L. *J. Am. Chem. Soc.* **1938**, *60*, 1846.
14. Brauer, B.; Sleater, G. *J. Less-Common Met.* **1970**, *21*, 283.
15. Ferrari, A.; Tani, E. *Gazz. Chim. Ital.* **1959**, *89*, 502.
16. Hoffmann, R. *J. Chem. Phys.* **1963**, *39*, 1397.
17. Ren, J.; Liang, W.; Whangbo, M.-H. *CAESAR*; Primecolor Software, Inc.: Cary, NC, 1999.
18. Klepp, K. O.; Bronger, W. *J. Less Common Met.* **1987**, *128*, 65.
19. Klepp, K. O.; Weithaler, C. *Z. Kristallogr.* **1998**, *213*, 18.
20. Klepp, K. O.; Bronger, W. *J. Less-Common Met.* **1987**, *132*, 173.
21. Szytula, A.; Penc, F. B.; Jezierski, A. *J. Alloys Comp.* **2001**, *317-318*, 340.
22. (a) McGuire, G. E.; SchWeitzer, G. K.; Carlson, T. A. *Inorg. Chem.* **1973**, *12*, 2450. (b) Briggs, D. In *Practical Surface Analysis*, 2nd Ed.; Briggs, D., Seah, M. P., Eds.; John Willey & Sons: New York, 1992; Vol. 1.